Applied Surface Science 464 (2019) 294–300

Contents lists available at ScienceDirect

Applied Surface Science

journal homepage: www.elsevier.com/locate/apsusc

Full Length Article

# Honeycomb porous carbon frameworks from wheat flour as supports for $Cu_xO$-$CeO_2$ monolithic catalysts

Shuang Wang, Lihui Yan, Yuansong Zhao, Yurong Ma, Guoqing Wu, Jinfang Wu*, Shanghong Zeng*

*Inner Mongolia Key Laboratory of Chemistry and Physics of Rare Earth Materials, School of Chemistry and Chemical Engineering, Inner Mongolia University, Hohhot 010021, China*

ARTICLE INFO

*Keywords:*
Honeycomb porous carbon
Monolithic catalysts
Small size effect
Oxygen vacancy
Preferential CO oxidation

ABSTRACT

The honeycomb porous carbon (HPC) material is prepared by one-step pyrolysis of the wheat flour, and then a series of $Cu_xO$-$CeO_2$/HPC monolithic catalysts are constructed via the hydrothermal method. It is found that the HPC support with interconnected porous structure and high BET surface area is capable of decreasing the particle sizes of copper species and ceria by preventing the agglomeration of nanoparticles. The small-sized $CeO_2$ particles on HPC surface facilitate the formation of a large amount of oxygen vacancies, which not only participate in oxygen activation and oxidation of carbon monoxide but also improve the redox reactivity of copper species and ceria. Thus the $Cu_xO$-$CeO_2$/HPC catalysts exhibit good catalytic performance in the CO-PROX reaction. Here, we address the use of low-cost and efficient carbon support in the catalytic reaction.

## 1. Introduction

Proton exchange membrane fuel cells (PEMFCs) are promising and eco-friendly power generators [1–3]. However, one technical problem should be solved during the application of the PEMFCs. The small quantity of CO in the hydrogen streams generated from the stream reforming of hydrocarbons and water-gas shift (WGS) must be reduced below 100 ppm in order to avoid poisoning the anodes of fuel cells [4,5]. The preferential CO oxidation (CO-PROX) is one of the most efficient methods for the purification of such $H_2$-rich streams, and CuO-$CeO_2$ oxides are prospective alternatives to expensive Pt or Au catalysts [6,7]. Nevertheless, the textural properties of CuO-$CeO_2$ oxides need to be improved considering the dispersion of active components.

Honeycomb-like porous carbon materials with high specific surface area, good conductivity, and interconnected diffusion channels have attracted attention as the supports or catalysts in several reactions, mainly due to their abundance and accessibility of the required raw materials [8–10]. In addition, the introduction of HPC could facilitate the dispersion of metal oxide particles to provide more active and nucleated sites. Moreover, the high electrical conductivity of carbon materials might enhance the synergistic effect between metal oxides.

Herein, we developed a feasible method to prepare the interconnected honeycomb-like porous carbon via one-step pyrolysis of the wheat flour. And then the $Cu_xO$-$CeO_2$/HPC monolithic catalysts were synthesized via a facile hydrothermal procedure. The multiple characterization techniques were used to study the effect of HPC support on the dispersion of active components and catalytic performance for CO-PROX reaction.

## 2. Experimental

### 2.1. Catalyst preparation

All of the chemicals used in our experiments are of analytical grade and no further purification. Cerium(III) nitrate hexahydrate (99.9%) and copper(II) nitrate (98.0–102.0%) were purchased from Sinopharm Chemical Reagent Co., Ltd (Beijing, China). Ammonium hydroxide (96.0%) and absolute ethanol ($\geq$99.7%) were obtained from Tianjin Beilian Fine Chemical Development Company (Tianjin, China).

The honeycomb porous carbon material was prepared by one-step pyrolysis of the wheat flour. The 3 g wheat flour and 3 g KOH were ground together, and then calcined at 700 °C for 100 min in $N_2$ atmosphere in a tubular furnace. The furnace was cooled down to room temperature naturally. The resulting material was treated with HCl to neutralize residual KOH, and then washed thoroughly with deionized water until the pH value was adjusted to approximate 7.0. After drying at 60 °C for 24 h, the material was ground into fine powder. The obtained carbon material was named as honeycomb porous carbon (HPC).

* Corresponding authors.
*E-mail addresses:* jfwu@imu.edu.cn (J. Wu), zengshanghong@imu.edu.cn (S. Zeng).

https://doi.org/10.1016/j.apsusc.2018.09.088
Received 25 July 2018; Received in revised form 10 September 2018; Accepted 10 September 2018
Available online 11 September 2018
0169-4332/ 

A series of $Cu_xO$-$CeO_2$/HPC monolithic catalysts were synthesized by a simple hydrothermal method. The $Cu(NO_3)_2·3H_2O$, $Ce(NO_3)_3·6H_2O$ and appropriate amounts of HPC were dissolved in 24 mL deionized water under constant stirring. The pH value of the mixture was adjusted to 10 using $NH_3·H_2O$ under air atmosphere. The solution was transferred to stainless steel autoclave for hydrothermal reaction at 80 °C for 4 h. The products were cooled down to room temperature and washed fully via deionized water and ethanol, and then were dried under vacuum at 60 °C for 24 h and calcined at 300 °C for 2 h in $N_2$ atmosphere. The obtained samples were denoted as $Cu_xO$-$CeO_2$/HPC. The similar method was used to prepare the $Cu_xO$/HPC, $CeO_2$/HPC and CuO-$CeO_2$ catalysts.

### 2.2. Catalyst characterization and activity tests

The contents of Cu and Ce in the calcined catalysts were determined by inductively coupled plasma emission spectroscopy (ICP-AES) at the Varian ICP-AES. The morphology and microstructure of the samples were obtained by a Hitachi S-4800 scanning electron microscope. Pt was sprayed on the surface in order to increase the conductivity of the samples. TEM and the HRTEM images of the samples were taken on a Tecnai G2 F20 S-Twin instrument with an acceleration voltage of 200 kV. The samples were dispersed in ethanol with the ultrasonic treatment. XPS spectra of the samples were performed on a Perkin Elmer PHI 5000 ESCT instrument with monochromatic Al Kα radiation (150 W, 1486.6 eV), where the spectra of samples were recorded with the constant pass energy values at 25 eV and the X-ray spot was 500 µm. Powder X-ray diffraction patterns were recorded on a PANalytical X'pert PRO diffractometer with Cu Kα source (λ = 0.15406 nm) in the range of $2\theta$ between 5 and 85°. The mean crystallite sizes were estimated from the Scherrer's equation. The textural properties were tested on the Quadrasorb evo physical adsorption apparatus. The surface area and pore size distribution were determined by the Brunauer-Emmett-Teller (BET) and the Barrette-Joynere-Halenda (BJH) methods, respectively. $H_2$ temperature-programmed reduction was conducted on a Micromeritics Apparatus (AutoChemII 2920). The reduction gas was 10% $H_2$/Ar gas mixture and the flow rate of gas was 50 mL·min$^{-1}$. The 100 mg sample was placed on top of some silica wool in a quartz reactor. Before reduction, the sample was pretreated at 200 °C for 1 h in a $N_2$ stream in order to remove the contaminants.

CO-PROX activity tests were carried out on a fixed bed reactor. The 100 mg sample and quartz sand with equal volume were evenly mixed in the quartz tube reactor. The reaction was carried out at atmospheric pressure with an airspeed of 40,000 mL $g_{cat}^{-1}$ $h^{-1}$. The range of reaction temperature was 35–215 °C, which was divided into 10 segments to collect information. The composition of reaction gasses was 1% CO, 1% $O_2$ and 50% $H_2$, $N_2$ (equilibrium gas). The inlet and outlet gas compositions were measured by a GC-2014C gas chromatograph. A 5A molecular sieve column was used to separate CO, $O_2$ and $N_2$. $CO_2$ was determined by a TDX-01 column. The conversion of CO and the $CO_2$ selectivity were calculated according to Eqs. (1) and (2):

$$C_{CO} = ([CO]_{in} - [CO]_{out})/[CO]_{in} \times 100\% \quad (1)$$

$$S_{CO_2} = 0.5([CO]_{in} - [CO]_{out})/([O_2]_{in} - [O_2]_{out}) \times 100\% \quad (2)$$

## 3. Results

### 3.1. Composition and catalytic performance

The ICP-AES data in Table 1 demonstrate that the theoretical Cu/Ce (molar ratio) has a certain deviation from those of actual values in the $Cu_xO$-$CeO_2$/HPC monolithic catalysts due to the application of hydrothermal method. In addition, the amount of HPC support is 40% in the $Cu_xO$-$CeO_2$/HPC monolithic catalysts.

Fig. 1 displays CO conversion and $CO_2$ selectivity over the as-prepared samples. It can be observed that the HPC, $Cu_xO$/HPC and $CeO_2$/HPC all exhibit poor catalytic activity for the CO-PROX reaction in comparison with the CuO-$CeO_2$ and $Cu_xO$-$CeO_2$/HPC monolithic catalysts, suggesting that the coexistence of copper oxide and ceria enables their interaction to produce the intriguing active sites toward the enhancement of catalytic activity for CO-PROX reaction. CO reacts with surface oxygen of ceria to produce $CO_2$ and leaves an oxygen vacancy in the Mars-van Krevelen mechanism [11]. Here, copper species can absorb CO, and ceria might promote copper species to change valence. Moreover, the $Cu_xO$-$CeO_2$/HPC monolithic catalysts show higher low-temperature catalytic activity and wider temperature window (135–195 °C) of complete CO conversion than the conventional CuO-$CeO_2$ catalyst, which might be attributed to the reduction property and the dispersion effect of HPC support on the active species. The HPC support facilitates the reduction of ceria to generate defects sites on ceria, which ensures the formation of active oxygen species at lower temperatures [11]. It is worth noting that the $Cu_xO$-$CeO_2$/HPC-B exhibits the best catalytic performance among the $Cu_xO$-$CeO_2$/HPC monolithic catalysts, especially at lower temperature. Moreover, the $Cu_xO$-$CeO_2$/HPC monolithic catalysts also exhibit higher $CO_2$ selectivity (> 75%) at the temperature of 100% CO conversion compared with the conventional copper-cerium oxide catalysts in the literature of 66% [12], 63% [13] and 40% [14].

**Table 1**
Composition and surface properties of the catalysts.

| Catalyst | Cu/Ce molar ratio[a] | Cu/Ce molar ratio[b] | $Ce^{3+}$ (%)[c] | $I_{sat}/I_{pp}$[c] | $V_O$ (%)[d] |
|---|---|---|---|---|---|
| $Cu_xO$-$CeO_2$/HPC-A | 1 | 0.98 | 17.22 | 0.33 | 4.55 |
| $Cu_xO$-$CeO_2$/HPC-B | 1:2 | 0.49 | 15.43 | 0.29 | 4.45 |
| $Cu_xO$-$CeO_2$/HPC-C | 2:1 | 1.96 | 18.31 | 0.43 | 4.73 |

[a] Theoretical value.
[b] By ICP-AES analysis.
[c] Calculated from XPS results.
[d] $[V_O] = (1 - (3\,[Ce^{3+}] + 4\,[Ce^{4+}])/4)$.

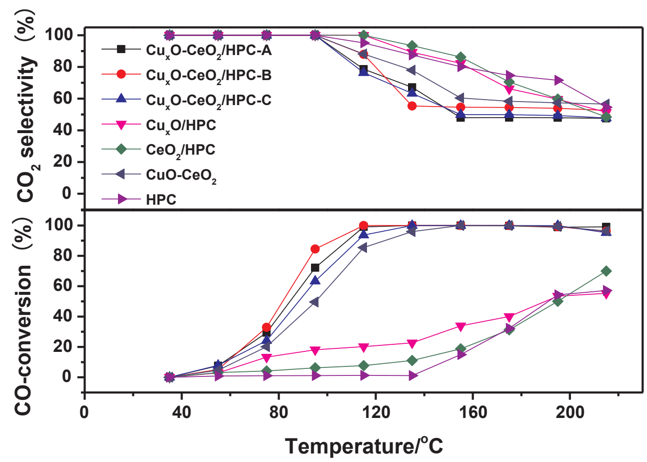


**Fig. 1.** CO conversion and $CO_2$ selectivity over the samples. (Feed composition: $[CO]_{in}$ = 1%, $[O_2]_{in}$ = 1%, $[H_2]_{in}$ = 50%, $N_2$ balance).

### 3.2. Morphology and surface compositions

Microstructural characteristics of the $Cu_xO$-$CeO_2$/HPC catalysts were investigated by SEM, TEM, HRTEM and SEM-EDS mapping. Fig. 2 displays SEM images of the HPC and $Cu_xO$-$CeO_2$/HPC monolithic catalysts. The HPC support presents honeycomb-shaped porous